Dalton Transactions

ROYAL SOCIETY OF CHEMISTRY

PAPER

View Article Online
View Journal | View Issue



Cite this: *Dalton Trans.*, 2023, **52**, 10927

# Catching up with tetrazines: coordination of Re(I) to 1,2,4-triazine facilitates an inverse electron demand Diels–Alder reaction with strained alkynes to a greater extent than in corresponding 1,2,4,5-tetrazines†

Mark Sims, [a] Sotiris Kyriakou,[a,b] Aidan Matthews,[a] Michael E. Deary [a] and Valery N. Kozhevnikov *[a]

Received 15th May 2023,
Accepted 19th July 2023

DOI: 10.1039/d3dt01451g

rsc.li/dalton

Inverse electron demand Diels Alder (IEDDA) reactions of 1,2,4-triazines are of interest to biorthogonal chemistry but suffer from slow kinetics. It is shown here that coordination of Re(I) to a 1,2,4-triazine ring speeds up the IEDDA reaction with bicyclooctyne (BCN) by a factor of 55. Comparative analysis with corresponding 1,2,4,5-tetrazine analogues reveals that the origin of the increased reactivity is markedly different and more profound than in tetrazine analogues. DFT calculations and subsequent analysis indicated the greater increase for the triazine than the tetrazines on coordination could be attributed to the triazine's lower distortion energy and more favourable interaction energy for the triazine, the latter attributable to lower Pauli repulsion than the tetrazines rather than to favourable frontier orbital energies.



## Introduction

Bioorthogonal chemistry relies on reactions that can be carried out in living systems, under physiological conditions.[1,2] Because of low concentrations of the reactants, a biorthogonal reaction should have very fast kinetics to be completed in meaningful timeframe. Inverse electron demand Diels Alder (IEDDA) [4 + 2] cycloadditions between 1,2,4,5-tetrazines and strained alkenes such as transcyclooctenes (TCO) or strained alkynes such as bicyclooctyne (BCN) are one of the fastest bioorthogonal reactions known to date.[3] These reactions have been adapted for a variety of applications from bioimaging to pre-targeted radiotherapy.[3] Unfortunately, almost inevitably, fast kinetics of the reaction is usually associated with low stability of the reagents.[4] There has been a significant research effort to develop diene systems with the aim of keeping a good balance between high kinetic rate constants of the IEDDA reaction and the stability of the reagents. For example, the introduction of a methyl group into 1,2,4,5-tetrazine significantly improves the stability under biological conditions.[4] Similarly, more stable 1,2,4-triazines can be used as dienes in IEDDA reactions with strained dienophiles[5] but in comparison to tetrazines, they are less electron deficient and therefore show comparatively lower reactivity.[6] One way to improve reactivity is to introduce electron-withdrawing groups in the triazine ring, but again this comes with a penalty in terms of stability.[6] Very recently Vrabel and co-workers introduced N1-alkyl-1,2,4-triazinium salts as an efficient diene system in reaction with BCN.[7]

Metal coordination is another way to facilitate the IEDDA reaction, and it was shown that both tetrazines and triazines react much faster in IEDDA reactions if directly coordinated to a metal ions. For example, Lo and co-workers were first to demonstrate this effect in tetrazine Ir(III) complexes.[8] Our group showed that the 1,2,4-triazine Ir(III) complexes react with BCN approximately 200 times faster than the corresponding uncoordinated ligands.[9] More recently, the boost of the reaction rates in Ru(II)[10,11] and Re(I)[12] complexes of tetrazines has also been demonstrated. Metal complexation not only facilitates the click reaction but also brings many opportunities for further modification of the structures and designing new methodologies in chemical biology. In one elegant example by Fox and co-workers a protein molecule was covalently tagged with pyridyl-tetrazine which is capable of coordination to nickel-iminodiacetate resin commonly used for His-tags. This coordination allowed not only the purification of the protein, but also quick and quantitative functionalisation of the protein by on-resin IEDDA reaction.[13] Importantly, transition

[a]*Department of Applied Sciences, Northumbria University, Newcastle upon Tyne, NE1 8ST, UK. E-mail: valery.kozhevnikov@northumbria.ac.uk*
[b]*Department of Cancer Genetics, Therapeutics & Ultrastructural Pathology, The Cyprus Institute of Neurology & Genetics, Ayios Dometios, 2371, Nicosia, Cyprus*
† Electronic supplementary information (ESI) available. See DOI: https://doi.org/10.1039/d3dt01451g

metal click-reagents provide unique metal-based properties that are useful for bio-imaging. For example, luminescent metal complexes are becoming increasingly popular in bio-imaging offering high photostability and possibilities to eliminate background autofluorescence by time-resolved techniques. Metal complexes of radioactive $^{99}$Tc are important in radio-imaging, while complexes of Mn(II) are under development as imaging probes in MRI.

In this paper we report a novel Re(I) complex of 1,2,4-triazine **6** and its performance as a potential bioorthogonal reagent. The corresponding tetrazine complexes **4** and **5** were evaluated for comparison. We primarily focus on examining reactivity of these complexes and the role metal coordination plays in boosting the rates of IEDDA reactions.

## Results and discussion

### Synthesis

All ligands used in this study have been previously reported. The tetrazine ligands **1** [14] and **2** [9] were prepared according to published procedures. The last step in the synthesis of the triazine ligand **3** [15] was optimised as follows. In our previous synthesis this dehydrazination step from **7** to **3** was performed by treatment compound **7** with sodium methoxide. The yield of this step was poor, and the reaction could not be successfully scaled up above 0.5 g. We therefore optimised the reaction by carrying out the dehydrazination step using manganese dioxide as an oxidising agent. The reaction on 3 g scale gave the desired triazine in 43% yield. The synthesis of the Re(I) complexes was relatively straightforward and required a simple heating under reflux of a toluene solution of equimolar amounts of the ligand and $Re(CO)_5Cl$. (Scheme 1) The yields are generally in the range of 70–90%. The synthesis of complex **4** was previously described.[12] The novel compounds are characterised by $^1$H, $^{13}$C NMR, IR and UV spectroscopy and high resolution mass spectrometry. The experimental procedures and analytical data can be found in ESI.†

### Analysis of NMR data

By careful analysis of the NMR data, including HSQC technique, we assigned all the signals in the $^{13}$C and $^1$H spectra in the coordinated and free ligands. The changes in chemical shifts of $^1$H and $^{13}$C atoms upon coordination to Re(I) can therefore been traced (Fig. S1†). Upon coordination, most of the signals in all compounds experience downfield shift. This may be a result of electron-withdrawing nature of the positively charged Re(I) ion. However, the degree of the changes varies significantly, indicating that the magnetic environment

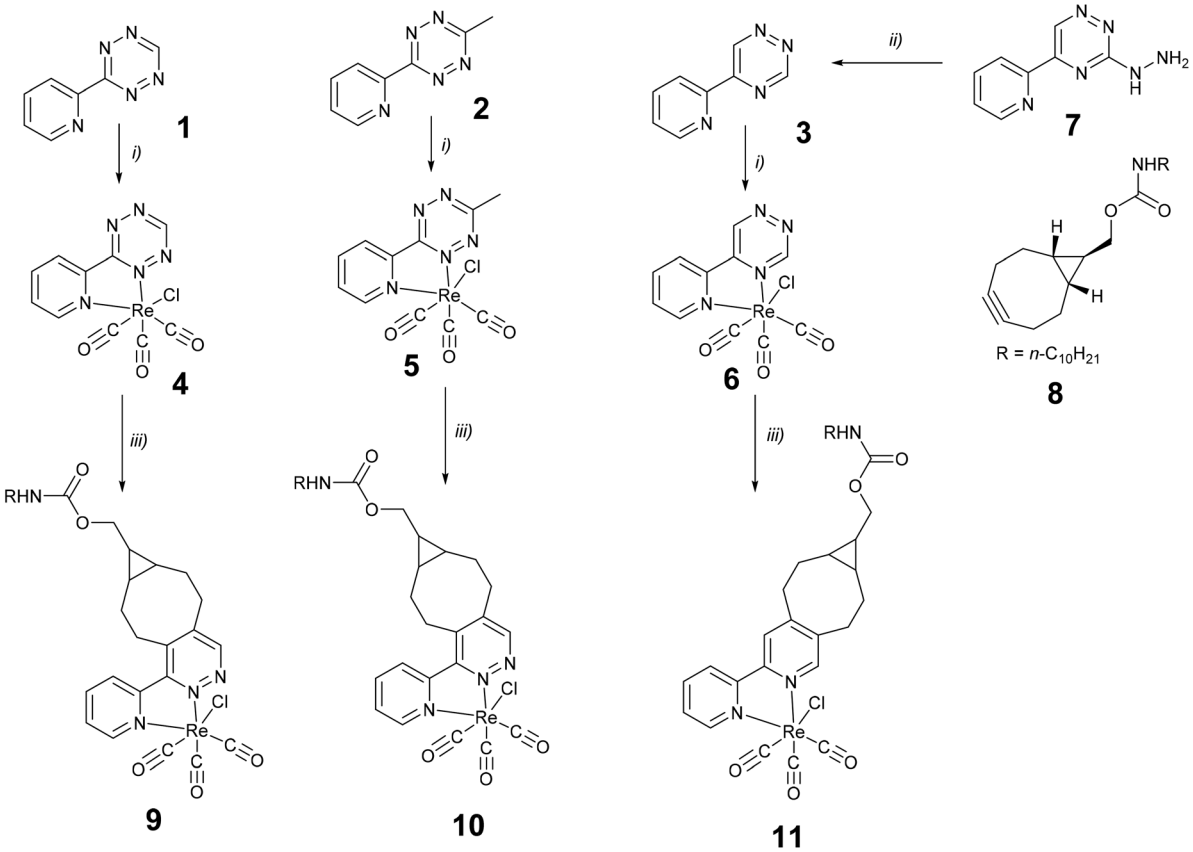


**Scheme 1** Synthesis of ligand **3** and metal complexes **4**–**6** used in this study as well as products of the IEDDA reactions with BCN-C10. Reaction conditions: (i) $Re(CO)_5Cl$, toluene, reflux, 2 hours, 76% (**4**), 76% (**5**), 87% (**6**); (ii) $MnO_2$, THF, 0 °C, 45 min, 43%; (iii) BCN-C10 **8**, methanol, RT.

around nuclei changes unevenly upon coordination. The magnetic environment, however, is influenced by many factors including anisotropic through-space effects and caution should be taken in correlating the NMR data with the reactivity of the dienes. In the diene systems, both in the tetrazine as well as in the triazine derivatives, the biggest changes are observed for the carbon atoms that are in *ortho*- positions to Re(I). Interestingly, the chemical shifts of carbons and protons of the pyridine ring in the triazine complex **6** are shifted more downfield in comparison with corresponding pyridine atoms in the tetrazine complexes. This is even though the tetrazine ring is more electron-deficient than the triazine one. The $^{13}C$ signals of the carbonyls are more difficult to assign and proposed assignment is somewhat speculative (Fig. S1†).

### Analysis of IR data

Sections of attenuated total reflectance IR spectra showing CO stretching vibrations of all complexes are depicted in Fig. S14.† There is sharp absorption at approximately 2024 $cm^{-1}$, the highest frequency of the CO stretches which according to DFT calculations arises primarily from the symmetric stretch of the CO groups trans to the diene ligand (see Fig. S31 and Table S3 in the ESI†). The other two CO stretching vibrations have very similar values and merge into a broad absorption band. The 1,2,4-triazine complex displayed this broad band at 1898 $cm^{-1}$, while for tetrazines the values are 1907 $cm^{-1}$. The lower CO stretching frequency in complex **6** suggests higher electron density on the central metal ion. This can be a result of better sigma-donation from the triazine ring or/and less back-donation of electron density from the metal to 1,2,4-triazine in comparison with 1,2,4,5-tetrazine analogue.

### Stability studies

The stability of the complexes **4–6** was studied by HPLC-MS at 37 °C in 10 mM MeCN/PBS (2 : 1) solution in the presence or absence of L-cysteine. As expected, the complex **4** formed by unsubstituted tetrazine, is the least stable in the series with half of the complex degraded in presence of cystein after 72 hours. Methyl substitution of the tetrazine significantly improves stability and the complex **5** is the most stable in the series. The triazine complex **6** is more stable than complex **4** but slightly less stable than **5**. It should be noted that stability of dienes is not compromised by Re(I) coordination.

### Cytotoxicity

A375, A431 and HaCaT cell viability levels were determined at 37 °C by utilizing the Alamar blue assay and summarised in Table S2.† For the tetrazine complexes **4, 5**, the introduction of the methyl group leads to significant increase in cytotoxicity, which is probably the result of more hydrophobic nature of the complex that leads to greater uptake of the complex **5** by cells. In comparison with tetrazines complexes, the triazine complex is less cytotoxic to A375 cells but shows similar or even greater toxicity to A431 and HaCaT cells. The data shows that, to satisfy the requirements of biorthogonality at 37 °C, the triazine complex **6** will not be toxic to the tested cells at concentrations of approximately 10 μM or lower for a typical overnight reaction.

### IEDDA reaction kinetics

The reaction between the BCN-derivative and tetrazine Re complexes or the corresponding ligand (the substrates) were carried out in methanol at 25 °C under pseudo-first order conditions (unless otherwise stated in the ESI†), with the BCN derivative in at least 10-fold excess. Reactions were followed by monitoring the loss of the substrate absorbance spectrophotometrically at a suitable wavelength (see ESI for further experimental details†). Observed pseudo-first-order rate constants, $k_{obs}$, were obtained using nonlinear regression of the monoexponential loss of absorbance with time. Second order rate constants, $k_2$, were obtained from the results of linear least squares carried out on plots of $k_{obs}$ against the concentration of the BCN derivative (see ESI†). The reactions were carried out using either an Applied Photophysics SX 17 stopped-flow spectrophotometer or a Pharmacia Ultraspec 2000 spectrophotometer depending on the rate of the reaction.

The data show that for the tetrazine complexes the increase in the reaction rate is approximately three-fold when compared with the respective ligands alone, whereas the reaction rate in the triazine complex is increased 56 times. Therefore, the Re(I) coordination effect is much more profound in the triazine dienophile in comparison with tetrazines. To understand the origin of such difference we carried out computational analysis.

## Computational analysis

Calculated activation energies for the reactions of the different dienes with BCN-C1-*anti* (*n*-decyl substituent was truncated to just methyl one) are listed in Table 1 and shown plotted against experimentally derived values in Fig. S32.† Within the Re complexes and within the free ligands, the experimental activation trends are matched by the calculations. All complexed ligands are calculated to have lower activation energies

**Table 1** Second order rate constants ($k_2$) for the reactions of dienes **1–6** with BCN-C10 dienophile **8** together with experimental and calculated activation energies for the reactions with **8**

| | | $G^{\ddagger}$/kJ mol$^{-1}$ | | $G^{\ddagger}$ (complex) − $G^{\ddagger}$ (ligand)/kJ mol$^{-1}$ | |
|---|---|---|---|---|---|
| Diene | $k_2$ [a]/M$^{-1}$ s$^{-1}$ | Exp. | Calc.[b] | Exp. | Calc. |
| **1** | 2367 ± 225 | 53.8 | 72.3 | — | — |
| **2** | 3.59 ± 0.18 | 69.9 | 89.6 | — | — |
| **3** | 0.0295 ± 0.0021 | 81.8 | 104.6 | — | — |
| **4** | 7523 ± 633 (×3) | 50.9 | 58.6 | −2.9 | −13.7 |
| **5** | 12.09 ± 0.12 (×3) | 66.8 | 82.1 | −3.0 | −7.4 |
| **6** | 1.644 ± 0.08 (×56) | 71.8 | 87.4 | −10.0 | −17.2 |

[a] Reactions were carried out in methanol at 25 °C using BCN-C10 as a dienophile. [b] Determined at the M06//LANL2DZ/6-311G(d,p) level (see ESI for details†).

than the respective free ligands, again consistent with experiment, and this drop in activation energy is most significant for the triazine reactions (**3**/**6**) both experimentally and according to the calculations. In each of **4**, **5** and **6**, the lowest-energy (gas-phase) transition state was found to be that corresponding to attack of the BCN from the Cl side of the diene as shown in Fig. 1.

The distortion-interaction model was used to gain additional insight into the calculated transition states, and the distortion and interactions energies are listed in Table 2 as well as shown plotted in Fig. 1. These values show that all dienes and dienophiles are calculated to have a greater distortion energy in the Re complex reactions than in the reactions of the free ligands. This difference is most significant for the dienes and may be attributable to their relative lack of flexibility when coordinated to Re. The total difference in distortion energy between complexed and free ligands is significantly greater (12.7 kJ $mol^{-1}$ in both cases) for the tetrazine reactions than the triazine reaction, providing an indication as to why the observed acceleration on complexation is most significant for the triazine reaction.

The calculated interaction energies are all significantly lower (>20 kJ $mol^{-1}$) for the Re-complexed ligands than the respective free ligands, consistent with the increased reaction rates on complexation. This decrease is greatest for the triazine ligand by *ca.* 10 kJ $mol^{-1}$, again providing a rationale for the greater observed increase in reaction rate of the triazine ligand upon coordination. A favourable interaction energy is often attributable to close matching of frontier orbital energies. For the compounds studied in this work the energy gaps between the frontier orbitals were all shown to decrease on complexation, consistent with more negative interaction energies, but the decrease in energy gap was consistent between the tetrazines and the triazine (all −1.00 ± 0.05 eV), suggesting orbital energies are not responsible for the larger calculated change in interaction energy for the triazine than the tetrazines. Visualisations of the interacting orbitals and values of the orbital energies are provided in Fig. S33 and Table S4 in the ESI.†

Energy decomposition analysis can give greater insights into underlying contributions and was carried out for the lowest-energy transition state calculated for each reaction. The values of the contributing terms are listed in Table S5 in the ESI† and the changes of interaction energy on complexation are shown in Fig. 2. The most significant favourable interaction on complexation for the tetrazines is calculated to be

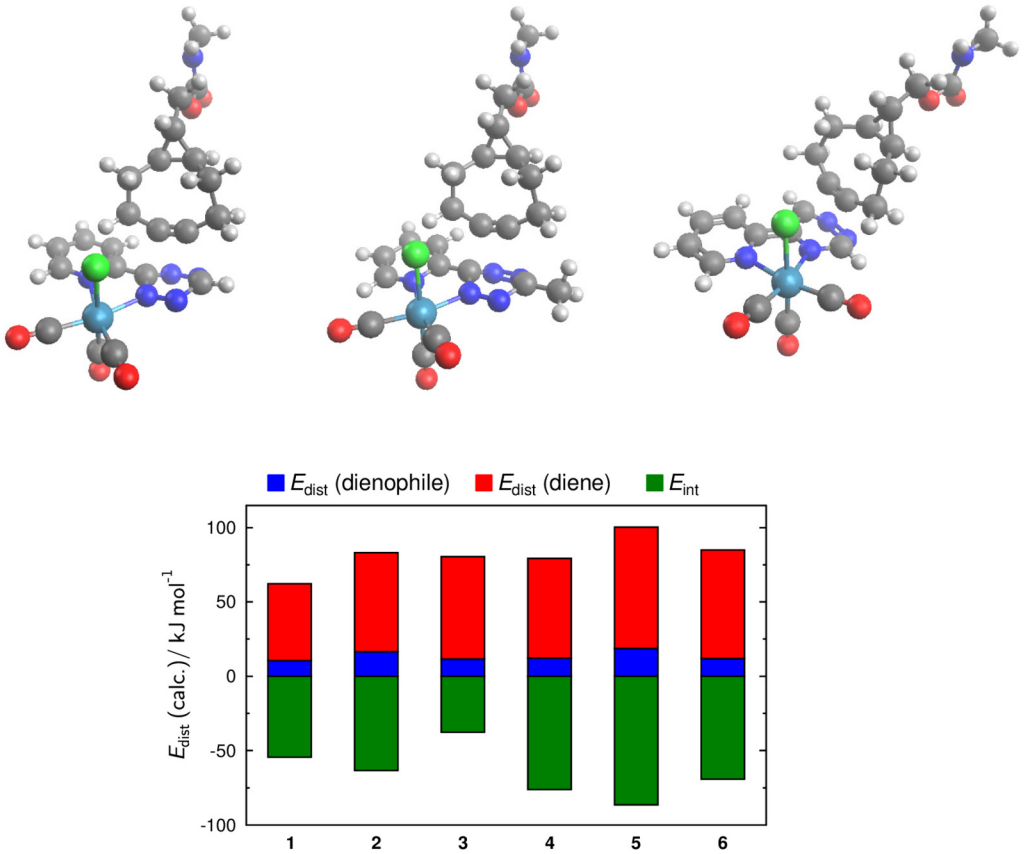


**Fig. 1** Transition state geometries of IEDDA reactions of complexes **4** (left), **5** (middle), **6** (right) with BCN-C1-*anti* and calculated distortion and interaction energies obtained from the transition states of the dienes with BCN-C1-*anti*.

Table 2 Distortion energies of the reactants in the calculated transition state geometries, interaction energies, and their differences, $\Delta E_{dist}$ and $\Delta E_{int}$, between complexed and free ligands

| | $E_{dist}$/kJ mol$^{-1}$ | | | $\Delta E_{dist}$/kJ mol$^{-1}$ | | | $E_{int}$/kJ mol$^{-1}$ | |
|---|---|---|---|---|---|---|---|---|
| Diene | Dienophile | Diene | Total | Dienophile | Diene | Total | | |
| **1** | 10.6 | 51.6 | 62.2 | | | | −54.5 | |
| **2** | 16.6 | 66.6 | 83.2 | | | | −63.5 | |
| **3** | 11.7 | 68.9 | 80.5 | | | | −37.7 | |
| **4** | 12.3 | 67.0 | 79.3 | 1.7 | 15.4 | 17.1 | −76.1 | −21.6 |
| **5** | 18.8 | 81.6 | 100.4 | 2.2 | 14.9 | 17.1 | −86.4 | −23.0 |
| **6** | 12.0 | 73.0 | 85.0 | 0.3 | 4.1 | 4.4 | −69.3 | −31.7 |

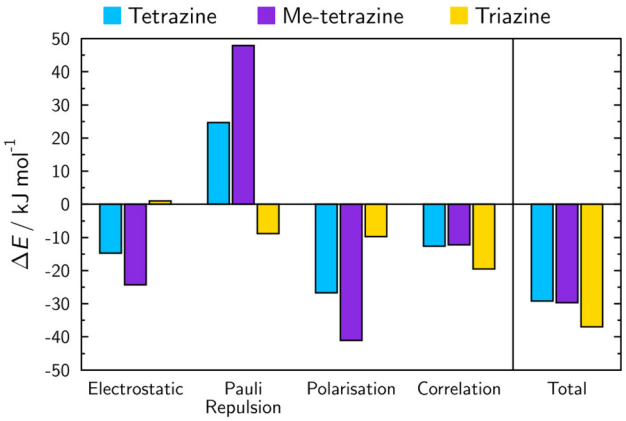


Fig. 2 Energy decomposition analysis of the change in interaction energies, $\Delta E$, on complexation, defined as the difference in the respective energy term of the Re complex and the free ligand with BCN-*anti*.

the polarisation, consistent with a previous report on the reaction of **4** with styrene.[16] When compared with the tetrazines the behaviour of the triazine is quite different, with electrostatic interactions and Pauli repulsion exhibiting the opposite trends to the tetrazines. The most significant difference between the tetrazine and triazine in terms of the change on complexation is the Pauli repulsion, which exhibits a large increase for the tetrazines, but a decrease for the triazine.

Quantum theory of atoms in molecule (QTAIM) analysis was used to integrate the electron density associated with each of the C and N atoms in the aromatic rings comprising the dienes. The differences in the total electron density on the tetrazine rings on complexation were calculated to be +0.122 and +0.084 for **1**/**4** and **2**/**5**, respectively, whereas the change for the triazine rings in compounds **3**/**6** was calculated as −0.048. This result indicates that the tetrazine rings exhibit a net gain of electron density on complexation, whereas the triazine exhibits a net loss, providing a rationale for the greater acceleration of the triazine reactions than the tetrazines. This result was further supported by orbital analysis of the diene orbitals calculated to have greatest overlap with the BCN orbitals, which were shown to increase in size on complexation for the tetrazines, and decrease in size on complexation for the triazine. Overlap integrals and visualisations of these orbitals are given in Table S6 and Fig. S35, S36 in the ESI.†

## Conclusion

In this contribution we investigated the effect of facilitating the IEDDA reaction of 1,2,4-triazines with BCN upon coordination to Re(I) and compared the effect with corresponding tetrazine analogues. We observed that the magnitude of the coordination affect is highest in the triazine pair **3**/**6** in comparison with tetrazine pairs **1**/**4** and **2**/**5**. IR data suggests that in comparison to 1,2,4,5-tetrazine, the 1,2,4-triazine experiences greater degree of depletion of electron density from the diene upon coordination. This is likely a result of better Sigma donation from the ligand and lesser back-donation from Re(I) centre to 1,2,4-triazine in comparison with 1,2,4,5-tetrazine. Computational analysis reveals significant differences in the origin of the metal coordination effect with most striking differences in Pauli repulsion that increases for the tetrazines but decreases for the triazine upon coordination. The improved kinetics and unique metal-based functionality render metal complexes of 1,2,4-triazines as a valuable addition to the toolbox of biorthogonal chemistry.

## Experimental part

### 5-(Pyridine-2-yl)-1,2,4-triazine 3 [9]

A solution of **7** (2.85 g, 14.6 mmol, 1.0 eq.) in THF (100 ml) was cooled to 0 °C by ice/water bath. Activated manganese(IV) oxide (7.62 g, 87.6 mmol, 6.0 eq.) was added is small portions at 0 °C over 15 min and the reaction mixture was stirred at 0 °C for 30 min. The mixture was filtered through Celite (2 cm) by suction and the filtrate was evaporated to dryness to give a crude product. The product was purified by silica gel column chromatography using 30% EtOAc : DCM mixture to give **3** (982 mg, 43%) as a bright yellow solid. $^1$H NMR (400 MHz, DMSO-D$_6$): $\delta$ 10.18 (d, $J$ = 1.8 Hz, 1H), 9.85 (d, $J$ = 1.8 Hz, 1H), 8.81 (d, $J$ = 4.1, 1H), 8.47 (br. d, $J$ = 8.2 Hz, 1H), 8.07 (ddd, $J$ = 1.8, 7.8 Hz, 1H), 7.65 (ddd, $J$ = 0.9, 4.6, 5.6 Hz, 1H). $^{13}$C NMR (100 MHz, DMSO-D$_6$): $\delta$ 157.8, 153.9, 151.6, 150.7, 147.5, 138.7, 127.7, 123.2. NMR data in CDCl$_3$ is identical to the previously published.[9] HRMS (ESI): $m/z$ calcd for [M + H] 159.06707, found 159.06644.

### Complex 6

To a solution of the ligand **3** (158 mg, 1 mmol) in toluene (15 mL), Re(CO)$_5$Cl (360 mg, 1 mmol) was added and the

mixture was heated under reflux for 2 hours. The mixture was allowed to cool to RT. The solid was filtered off, washed with toluene and petrol ether to give after drying the desired complex as a red solid. Yield 406 mg (87%) $^{1}$H NMR (400 MHz, DMSO-$D_6$): $\delta$ 10.70 (s, 1H), 10.22 (s, 1H), 9.15 (d, $J$ = 4.6 Hz, 1H), 9.08 (d, $J$ = 7.8 Hz, 1H), 8.46 (t, $J$ = 7.8, 1H), 7.98–7.95 (m, 1H). $^{13}$C NMR (100 MHz, DMSO-$D_6$): $\delta$ 197.7, 196.4, 188.2, 157.8, 155.1, 154.7, 152.2, 149.0, 141.1, 131.5, 128.2. $\nu_{max}$/cm$^{-1}$: 2023, 1898. HRMS (ESI): $m/z$ calcd for [M + H] 464.97643, found 464.97513.

## Conflicts of interest

There are no conflicts to declare.

## Acknowledgements

The authors acknowledge financial support from Northern Accelerator.

## References

1 E. Saxon and C. R. Bertozzi, *Science*, 2000, **287**, 2007–2010.
2 R. E. Bird, S. A. Lemmel, X. Yu and Q. A. Zhou, *Bioconjugate Chem.*, 2021, **32**, 2457–2479.
3 B. L. Oliveira, Z. Guo and G. J. L. Bernardes, *Chem. Soc. Rev.*, 2017, **46**, 4895–4950.
4 M. R. Karver, R. Weissleder and S. A. Hilderbrand, *Bioconjugate Chem.*, 2011, **22**, 2263–2270.
5 D. N. Kamber, Y. Liang, R. J. Blizzard, F. Liu, R. A. Mehl, K. N. Houk and J. A. Prescher, *J. Am. Chem. Soc.*, 2015, **137**, 8388–8391.
6 F.-G. Zhang, Z. Chen, X. Tang and J.-A. Ma, *Chem. Rev.*, 2021, **121**, 14555–14593.
7 S. B. V. Šlachtová, A. La-Venia, J. Galeta, M. Dračínský, K. Chalupský, H. Mertlíková-Kaiserová, P. Rukovanský, R. Dzijak and M. Vrabel, *Angew. Chem., Int. Ed.*, 2023, DOI: **10.1002/anie.202306828**.
8 T. S.-M. Tang, H.-W. Liu and K. K.-W. Lo, *Chem. Commun.*, 2017, **53**, 3299–3302.
9 V. N. Kozhevnikov, M. E. Deary, T. Mantso, M. I. Panayiotidis and M. T. Sims, *Chem. Commun.*, 2019, **55**, 14283–14286.
10 M. Schnierle, M. Leimkühler and M. R. Ringenberg, *Inorg. Chem.*, 2021, **60**, 6367–6374.
11 C. Müller, P. Wintergerst, S. S. Nair, N. Meitinger, S. Rau and B. Dietzek-Ivanšić, *J. Photochem. Photobiol.*, 2022, **11**, 100130.
12 M. Schnierle, S. Blickle, V. Filippou and M. R. Ringenberg, *Chem. Commun.*, 2020, **56**, 12033–12036.
13 S. L. Scinto, T. R. Reagle and J. M. Fox, *Angew. Chem., Int. Ed.*, 2022, **61**, e202207661.
14 Y. Qu, F.-X. Sauvage, G. Clavier, F. Miomandre and P. Audebert, *Angew. Chem., Int. Ed.*, 2018, **57**, 12057–12061.
15 R. M. Versteegen, R. Rossin, W. ten Hoeve, H. M. Janssen and M. S. Robillard, *Angew. Chem., Int. Ed.*, 2013, **52**, 14112–14116.
16 A. Turlik, K. N. Houk and D. Svatunek, *J. Org. Chem.*, 2021, **86**, 13129–13133.